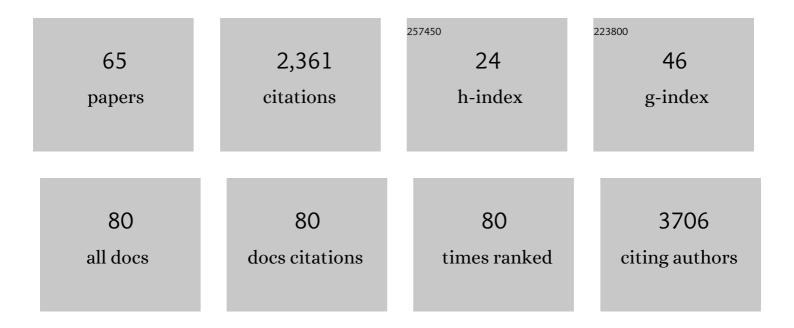
## Franklin I Aigbirhio

List of Publications by Year in descending order

Source: https://exaly.com/author-pdf/2132971/publications.pdf Version: 2024-02-01



#	Article	IF	CITATIONS
1	Evaluation of the Sensitivity and Specificity of <sup>11</sup> C-Metomidate Positron Emission Tomography (PET)-CT for Lateralizing Aldosterone Secretion by Conn's Adenomas. Journal of Clinical Endocrinology and Metabolism, 2012, 97, 100-109.	3.6	203
2	Intrinsic Activated Microglia Map to the Peri-infarct Zone in the Subacute Phase of Ischemic Stroke. Stroke, 2006, 37, 1749-1753.	2.0	163
3	Functionalized Bis(thiosemicarbazonato) Complexes of Zinc and Copper:Â Synthetic Platforms Toward Site-Specific Radiopharmaceuticals. Inorganic Chemistry, 2007, 46, 465-485.	4.0	134
4	Hypoxia and tissue destruction in pulmonary TB. Thorax, 2016, 71, 1145-1153.	5.6	133
5	Pathophysiologic Mechanisms of Cerebral Ischemia and Diffusion Hypoxia in Traumatic Brain Injury. JAMA Neurology, 2016, 73, 542.	9.0	125
6	A positron emission tomography study of nigro-striatal dopaminergic mechanisms underlying attention: implications for ADHD and its treatment. Brain, 2013, 136, 3252-3270.	7.6	90
7	Cellular confocal fluorescence studies and cytotoxic activity of new Zn(ii) bis(thiosemicarbazonato) complexes. Dalton Transactions, 2008, , 2107.	3.3	83
8	White Matter Perivascular Spaces on Magnetic Resonance Imaging. Stroke, 2015, 46, 1707-1709.	2.0	77
9	[ <sup>18</sup> F]AV-1451 binding in vivo mirrors the expected distribution of TDP-43 pathology in the semantic variant of primary progressive aphasia. Journal of Neurology, Neurosurgery and Psychiatry, 2018, 89, 1032-1037.	1.9	77
10	Designing Zn(ii) and Cu(ii) derivatives as probes for in vitro fluorescence imaging. Dalton Transactions, 2007, , 4988.	3.3	72
11	Neuroinflammation and protein aggregation co-localize across the frontotemporal dementia spectrum. Brain, 2020, 143, 1010-1026.	7.6	68
12	Neuroimaging of Inflammation in Memory and Related Other Disorders (NIMROD) study protocol: a deep phenotyping cohort study of the role of brain inflammation in dementia, depression and other neurological illnesses. BMJ Open, 2017, 7, e013187.	1.9	65
13	Imaging of Brain Hypoxia in Permanent and Temporary Middle Cerebral Artery Occlusion in the Rat using 18F-Fluoromisonidazole and Positron Emission Tomography: A Pilot Study. Journal of Cerebral Blood Flow and Metabolism, 2007, 27, 679-689.	4.3	62
14	Synaptic Loss in Primary Tauopathies Revealed by [ <scp><sup>11</sup>C</scp> ] <scp>UCBâ€J</scp> Positron Emission Tomography. Movement Disorders, 2020, 35, 1834-1842.	3.9	61
15	Dissociable Rate-Dependent Effects of Oral Methylphenidate on Impulsivity and D <sub>2/3</sub> Receptor Availability in the Striatum. Journal of Neuroscience, 2015, 35, 3747-3755.	3.6	54
16	In Vitro and In Vivo Evaluations of a Hydrophilic <sup>64</sup> Cu-Bis(Thiosemicarbazonato)–Glucose Conjugate for Hypoxia Imaging. Journal of Nuclear Medicine, 2008, 49, 1862-1868.	5.0	51
17	Spatial and Temporal Pattern of Ischemia and Abnormal Vascular Function Following Traumatic Brain Injury. JAMA Neurology, 2020, 77, 339.	9.0	49
18	Successful treatment of residual pituitary adenoma in persistent acromegaly following localisation by 11C-methionine PET co-registered with MRI. European Journal of Endocrinology, 2016, 175, 485-498.	3.7	41

Franklin I Aigbirhio

#	Article	IF	CITATIONS
19	Neuroinflammation predicts disease progression in progressive supranuclear palsy. Journal of Neurology, Neurosurgery and Psychiatry, 2021, 92, 769-775.	1.9	40
20	Characterizing infarction and selective neuronal loss following temporary focal cerebral ischemia in the rat: A multi-modality imaging study. Neurobiology of Disease, 2013, 51, 120-132.	4.4	38
21	Synthesis and Initial <i>in Vivo</i> Studies with [ <sup>11</sup> C]SB-216763: The First Radiolabeled Brain Penetrative Inhibitor of GSK-3. ACS Medicinal Chemistry Letters, 2015, 6, 548-552.	2.8	38
22	Neuroinflammation and Tau Colocalize in vivo in Progressive Supranuclear Palsy. Annals of Neurology, 2020, 88, 1194-1204.	5.3	38
23	Is neural activation within the rescued penumbra impeded by selective neuronal loss?. Brain, 2013, 136, 1816-1829.	7.6	28
24	In vivo evidence for preâ€symptomatic neuroinflammation in a <scp>MAPT</scp> mutation carrier. Annals of Clinical and Translational Neurology, 2019, 6, 373-378.	3.7	27
25	Synaptic density in carriers of C9orf72 mutations: a [ <sup>11</sup> C]UCBâ€J PET study. Annals of Clinical and Translational Neurology, 2021, 8, 1515-1523.	3.7	27
26	Rapid preparation of [11C]flumazenil: captive solvent synthesis combined with purification by analytical sized columns. Journal of Labelled Compounds and Radiopharmaceuticals, 2007, 50, 19-24.	1.0	24
27	Radiosynthesis and characterization of astemizole derivatives as lead compounds toward PET imaging of Ĩ"-pathology. MedChemComm, 2013, 4, 852.	3.4	24
28	Synthesis, in Vitro Evaluation, and Radiolabeling of Fluorinated Puromycin Analogues: Potential Candidates for PET Imaging of Protein Synthesis. Journal of Medicinal Chemistry, 2016, 59, 9422-9430.	6.4	23
29	Radiosynthesis of ( <i>R</i> , <i>S</i> )â€{ <sup>18</sup> F]GE387: A Potential PET Radiotracer for Imaging Translocator Protein 18â€kDa (TSPO) with Low Binding Sensitivity to the Human Gene Polymorphism rs6971. ChemMedChem, 2019, 14, 982-993.	3.2	22
30	Targeted Molecular Imaging in Adrenal Disease—An Emerging Role for Metomidate PET-CT. Diagnostics, 2016, 6, 42.	2.6	21
31	Molecular pathology and synaptic loss in primary tauopathies: an 18F-AV-1451 and 11C-UCB-J PET study. Brain, 2022, 145, 340-348.	7.6	21
32	An Efficient Method for Enhancing the Reactivity and Flexibility of [ <sup>18</sup> F]Fluoride Towards Nucleophilic Substitution Using Tetraethylammonium Bicarbonate. European Journal of Organic Chemistry, 2014, 2014, 6145-6149.	2.4	20
33	Insula serotonin 2A receptor binding and gene expression contribute to serotonin transporter polymorphism anxious phenotype in primates. Proceedings of the National Academy of Sciences of the United States of America, 2019, 116, 14761-14768.	7.1	20
34	An automated method for regular productions of copper-64 for PET radiopharmaceuticals. Inorganica Chimica Acta, 2010, 363, 1316-1319.	2.4	19
35	Validation of reference tissue modelling for [11C]flumazenil positron emission tomography following head injury. Annals of Nuclear Medicine, 2011, 25, 396-405.	2.2	19
36	11C-UCB-J synaptic PET and multimodal imaging in dementia with Lewy bodies. European Journal of Hybrid Imaging, 2020, 4, 25.	1.5	18

FRANKLIN I AIGBIRHIO

#	Article	IF	CITATIONS
37	Single-subject statistical mapping of acute brain hypoxia in the rat following middle cerebral artery occlusion: A microPET study. Experimental Neurology, 2011, 229, 251-258.	4.1	17
38	In vivo coupling of dendritic complexity with presynaptic density in primary tauopathies. Neurobiology of Aging, 2021, 101, 187-198.	3.1	17
39	A fluorescent molecular imaging probe with selectivity for soluble tau aggregated protein. Chemical Science, 2020, 11, 4773-4778. Comparison of Lorazepam	7.4	16
40	[7-Chloro-5-(2-chlorophenyl)-1,3-dihydro-3-hydroxy-2H-1,4-benzodiazepin-2-one] Occupancy of Rat Brain <sup>[3</sup> -Aminobutyric AcidA Receptors Measured Using in Vivo [3H]Flumazenil (8-Fluoro) Tj ETQqO 0 0 rgBT /Overlock and [11C]Flumazenil Micro-Positron Emission Tomography. Journal of Pharmacology and Experimental	10 Tf 50	622 Td (5,6-di 15
41	Therapeutics, 2007, 320, 1030-1037. A comparison of four PET tracers for brain hypoxia mapping in a rodent model of stroke. Nuclear Medicine and Biology, 2013, 40, 338-344.	0.6	15
42	Automated radiosynthesis of [ <sup>11</sup> C]UCBâ€J for imaging synaptic density by positron emission tomography. Journal of Labelled Compounds and Radiopharmaceuticals, 2020, 63, 151-158.	1.0	15
43	Imaging tau burden in dementia with Lewy bodies using [18F]-AV1451 positron emission tomography. Neurobiology of Aging, 2021, 101, 172-180.	3.1	14
44	Detection and Characterization of Small Molecule Interactions with Fibrillar Protein Aggregates Using Microscale Thermophoresis. ACS Chemical Neuroscience, 2017, 8, 2088-2095.	3.5	13
45	Synthesis, Radiolabelling and In Vitro Imaging of Multifunctional Nanoceramics. ChemNanoMat, 2018, 4, 361-372.	2.8	13
46	DJ-1 can form $\hat{l}^2$ -sheet structured aggregates that co-localize with pathological amyloid deposits. Neurobiology of Disease, 2020, 134, 104629.	4.4	13
47	Preclinical evaluation of (S)-[18F]GE387, a novel 18-kDa translocator protein (TSPO) PET radioligand with low binding sensitivity to human polymorphism rs6971. European Journal of Nuclear Medicine and Molecular Imaging, 2021, 49, 125-136.	6.4	11
48	Quantification of receptor–ligand binding potential in sub-striatal domains using probabilistic and template regions of interest. NeuroImage, 2011, 55, 101-112.	4.2	10
49	Flixotideâ"¢-pressurized metered-dose inhalers loaded with[18F]fluticasone propionate particles for drug deposition studies in humans with PET–formulation and analysis. Journal of Labelled Compounds and Radiopharmaceuticals, 2004, 47, 55-70.	1.0	9
50	InÂVivo <sup>18</sup> F-Flortaucipir PET Does Not Accurately Support the Staging of Progressive Supranuclear Palsy. Journal of Nuclear Medicine, 2022, 63, 1052-1057.	5.0	9
51	Synthesis and Assessment of Novel Probes for Imaging Tau Pathology in Transgenic Mouse and Rat Models. ACS Chemical Neuroscience, 2021, 12, 1885-1893.	3.5	8
52	[11C]PK11195-PET Brain Imaging of the Mitochondrial Translocator Protein in Mitochondrial Disease. Neurology, 2021, 96, e2761-e2773.	1.1	7
53	Mapping the binding site topology of amyloid protein aggregates using multivalent ligands. Chemical Science, 2021, 12, 8892-8899.	7.4	6
54	[ <i>Carboxyl</i> â€ <sup>11</sup> C]Labelling of Four Highâ€Affinity cPLA2α Inhibitors and Their Evaluation as Radioligands in Mice by Positron Emission Tomography. ChemMedChem, 2018, 13, 138-146.	3.2	5

Franklin I Aigbirhio

#	Article	IF	CITATIONS
55	Radiosynthesis of Carbon-11 Labeled Puromycin as a Potential PET Candidate for Imaging Protein Synthesis <i>in Vivo</i> . ACS Medicinal Chemistry Letters, 2016, 7, 647-651.	2.8	4
56	Assessing the Effects of Cytoprotectants on Selective Neuronal Loss, Sensorimotor Deficit and Microglial Activation after Temporary Middle Cerebral Occlusion. Brain Sciences, 2019, 9, 287.	2.3	4
57	A simple and efficient automated cGMP ompliant radiosynthesis of [ <sup>11</sup> C]metomidate using solid phase extraction cartridge purification. Journal of Labelled Compounds and Radiopharmaceuticals, 2019, 62, 190-197.	1.0	4
58	13th IIS(UK group) symposium. Journal of Labelled Compounds and Radiopharmaceuticals, 2004, 47, 299-334.	1.0	3
59	Effects of hyperoxia on 18F-fluoro-misonidazole brain uptake and tissue oxygen tension following middle cerebral artery occlusion in rodents: Pilot studies. PLoS ONE, 2017, 12, e0187087.	2.5	3
60	David James Silvester. Journal of Labelled Compounds and Radiopharmaceuticals, 2013, 56, 338-339.	1.0	2
61	[18F]-AV-1451 binding in the substantia nigra as a marker of neuromelanin in Lewy body diseases. Brain Communications, 2021, 3, fcab177.	3.3	2
62	Synthesis of [18F]Fluoromisonidazole (1-(2-Hydroxy-3-[18F]Fluoropropyl)-2-Nitroimidazole, [18F]FMISO). , 0, , 41-49.		1
63	226†Reduced synaptic density in progressive supranuclear palsy and corticobasal syndrome, revealed by [11C]UCB-J PET. Journal of Neurology, Neurosurgery and Psychiatry, 2022, 93, A78.3-A78.	1.9	1
64	Chemistry of Nitrogen-13 and Oxygen-15. , 2005, , 119-140.		0
65	[ICâ€Pâ€155]: ESTABLISHMENT OF A PET RADIOTRACER NETWORK FOR DEMENTIA RESEARCH. Alzheimer's and Dementia, 2017, 13, P117.	0.8	0